Electronic Supporting Information

SERS and MALDI-TOF MS Based Plasma Exosome Profiling for Rapid Detection of Osteosarcoma

Zhenzhen Han,[a] Jia Yi,[a] Yi Yang,[a] Dandan Li,[a] Cheng Peng,[b] Shuping Long,[c] Xinyan Peng,[a] Yuhui Shen[b], Baohong Liu,[a] and Liang Qiao*[a]

1. Department of Chemistry, and Shanghai Stomatological Hospital, Fudan University, Shanghai 200000, China

2. Department of Orthopedics, Ruijin Hospital, Shanghai Jiao Tong University School of Medicine, Shanghai 200000, China

3. Department of Clinical Laboratory Medicine, Shanghai Tenth People's Hospital of Tongji University, Shanghai, China

* Corresponding author. E-mail: liang_qiao@fudan.edu.cn

Table of contents

Figure S1. Isolation of exosomes by UC. S3

Figure S2. NTA, concentration and purity of HeLa and MCF-7 exosomes. S4

Figure S3. Characterization of AuNPs. S5

Figure S4. Schematic illustration of exosomes detection on SERS substrate. S6

Figure S5. SERS signals of HeLa exosomes compared to the controls. S7

Figure S6. NTA measurement of plasma-derived exosomes. S8

Figure S7. Concentration and purity of plasma-derived exosomes. S9

Figure S8. SERS signals of plasma-derived exosomes compared to the controls. S10

Figure S9. SERS signals of plasma-derived exosomes and cosine similarity of the SERS spectra. S11

Figure S10. Hierarchical clustering of the SERS data of plasma-derived exosomes. S12

Figure S11. PLS-DA analysis of the SERS data of plasma-derived exosomes. S13

Figure S12 MALDI-TOF mass spectra of plasma-derived exosomes and cosine similarity of the MALDI-TOF mass spectra. S14

Figure S13. Hierarchical clustering of the MALDI-TOF data of plasma-derived exosomes. S15

Figure S14. PLS-DA of the MALDI data of plasma-derived exosomes. S16

Table S1. assignments of the major SERS peaks. S17

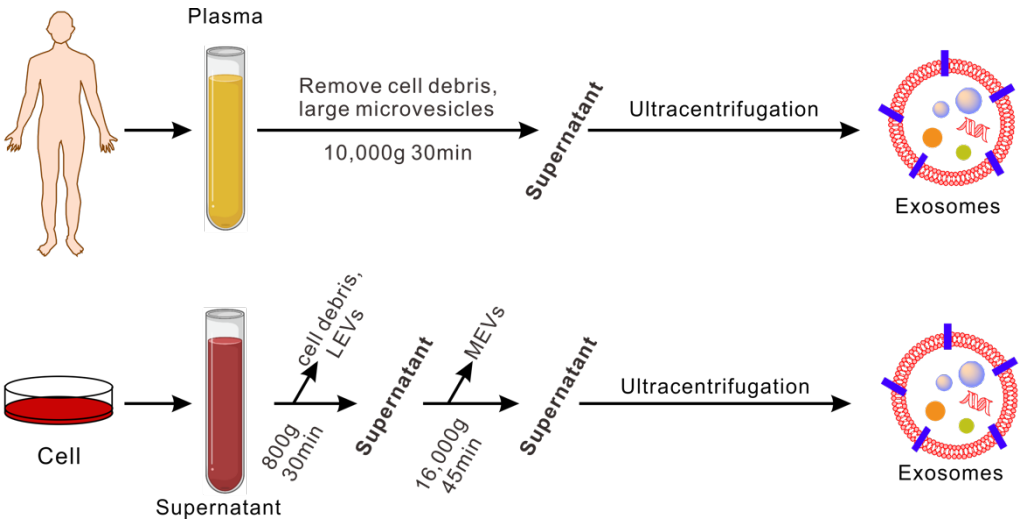

Figure S1. Isolation of LEVs, MEVs and exosomes from human plasma and cell supernatant.

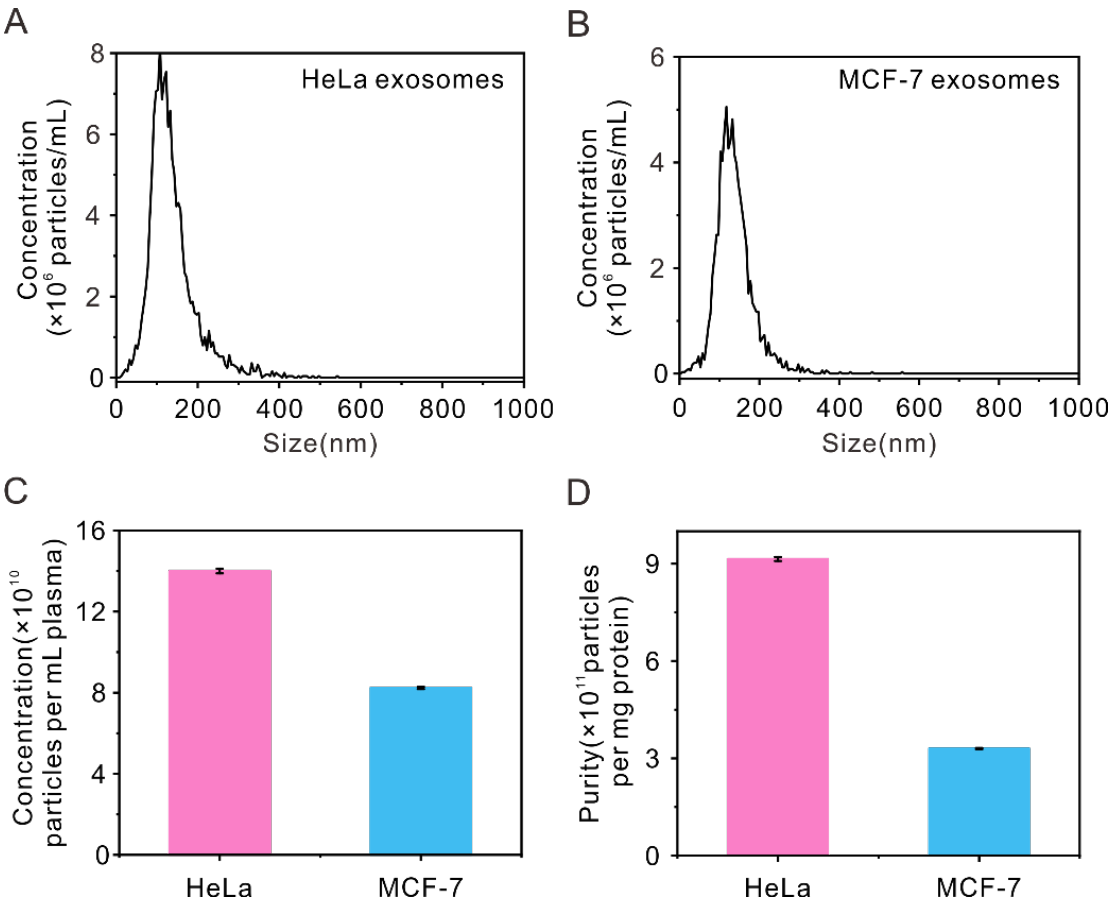

Figure S2. (A, B) NTA, (C) concentration and (D) purity analyses of HeLa and MCF-7 exosomes. The error bars represent the standard deviation of three replicates.

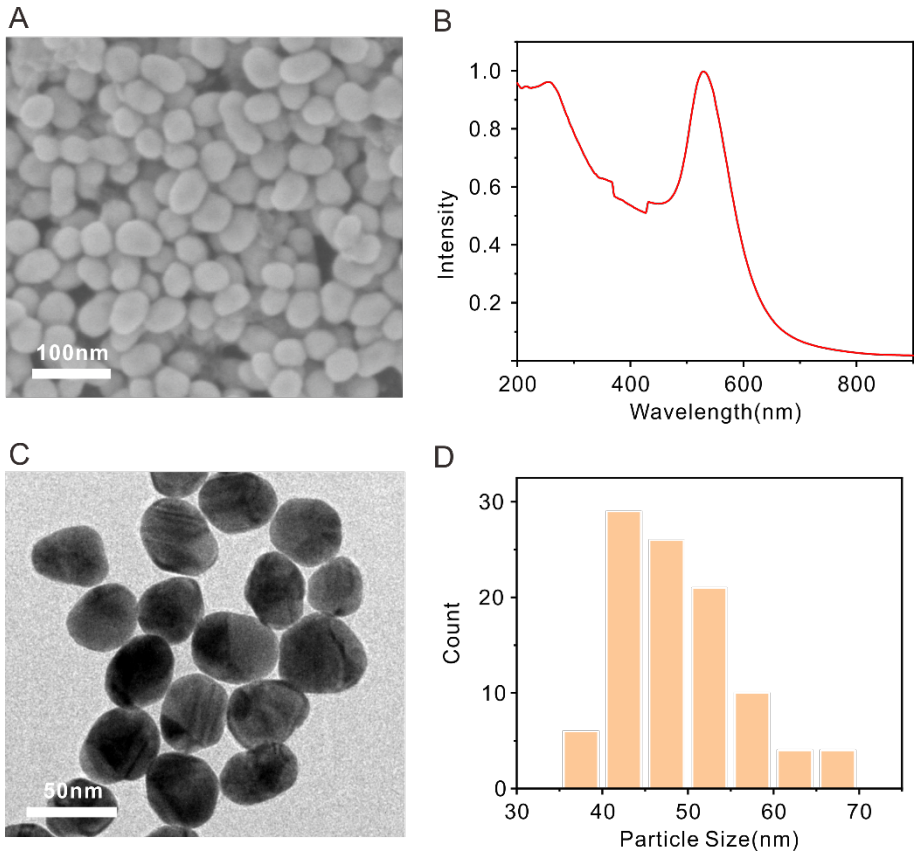

Figure S3. Characterization of AuNPs. (A) SEM image, (B) UV-vis spectra, (C) TEM image and (D) the particle size distribution.

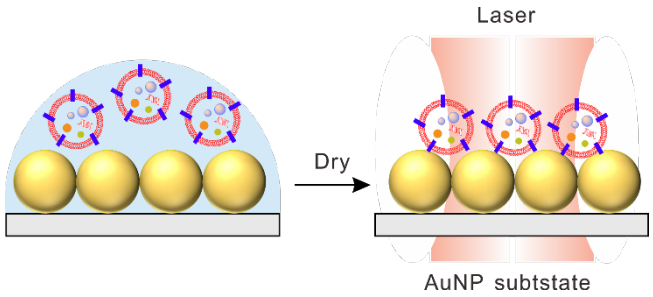

Figure S4. Schematic illustration of exosomes detection on SERS substrate.

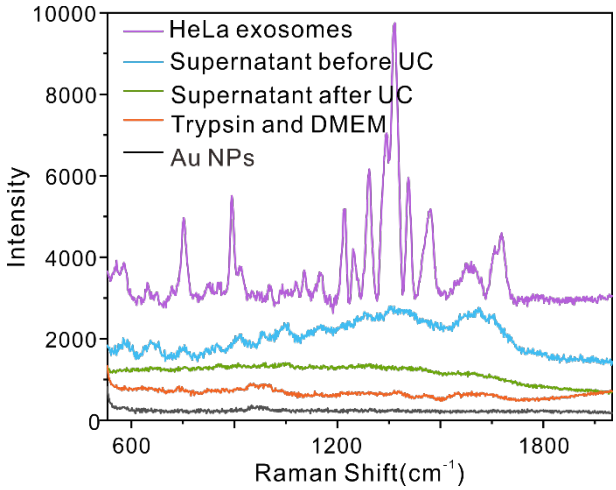

Figure S5. SERS signals of HeLa exosomes, HeLa cell supernatant before and after UC, the mixture of Trypsin and DMEM with 10% FBS, and the bare substrate of AuNPs.

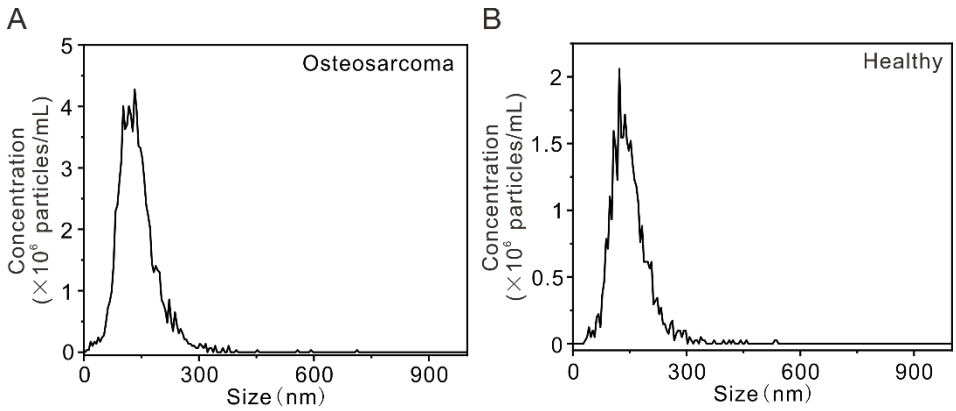

Figure S6. NTA measurement (200 times dilution) of the plasma-derived exosomes from (A) an osteosarcoma patient and (B) a healthy control.

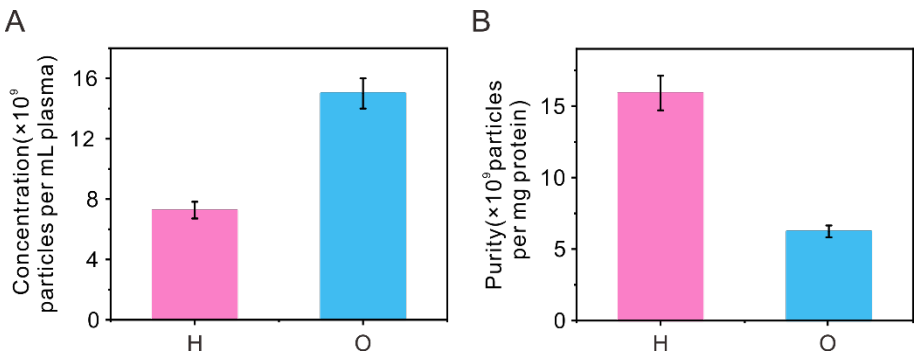

Figure S7. (A) Concentrations and (B) purities of exosomes isolated from the healthy control and the osteosarcoma patient. The error bars represent the standard deviation of three replicates.

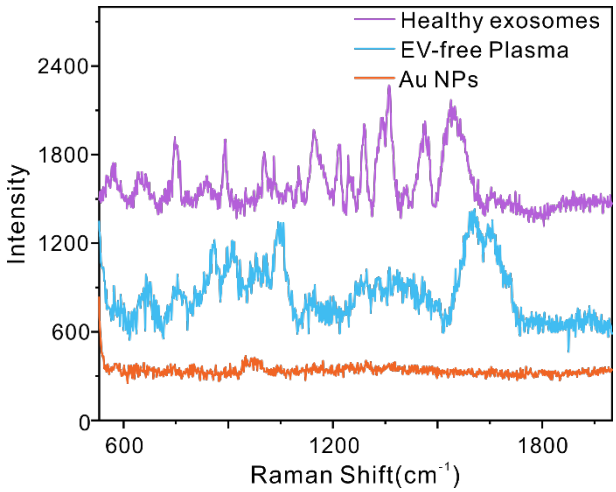

Figure S8. SERS signals of plasma-derived exosomes, EV-free plasma, and the bare substrate of AuNPs.

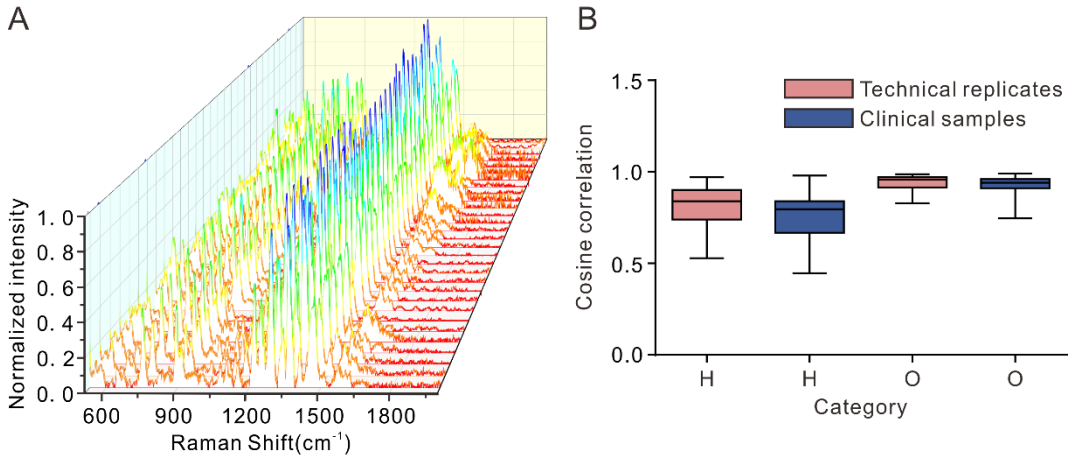

Figure S9. (A) The graph represents 30 representative SERS fingerprints of plasma-derived exosomes isolated from 10 osteosarcoma patients. Three replicates were performed for each sample. The adjacent three SERS fingerprints were from the same sample. (B) Cosine correlation of SERS fingerprints of plasma-derived exosomes isolated from 10 healthy controls (H) or 10 osteosarcoma patients (O). Three replicates were performed for each sample. The red box-plots represent the distribution of cosine correlation between technical replicates of each sample. The blue box-plots represent the distribution of cosine correlation of SERS fingerprints of different clinical samples. The boxes show interquartile ranges (IQR), and the whiskers show 95% percentiles; no outliers are shown.

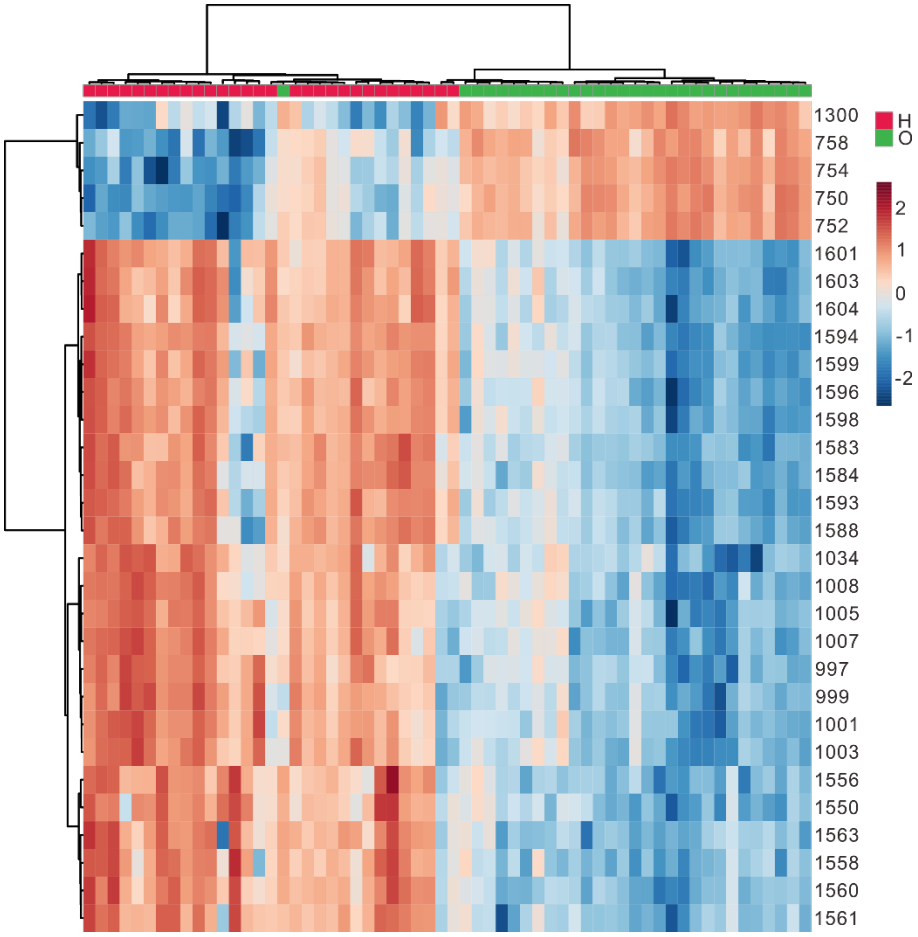

Figure S10. Hierarchical clustering of the SERS fingerprints of plasma-derived exosomes isolated from 10 healthy controls (H) and 10 osteosarcoma patients (O) shown as heatmap using Euclidean distance measure and Ward linkage. Three replicates were performed for each sample.

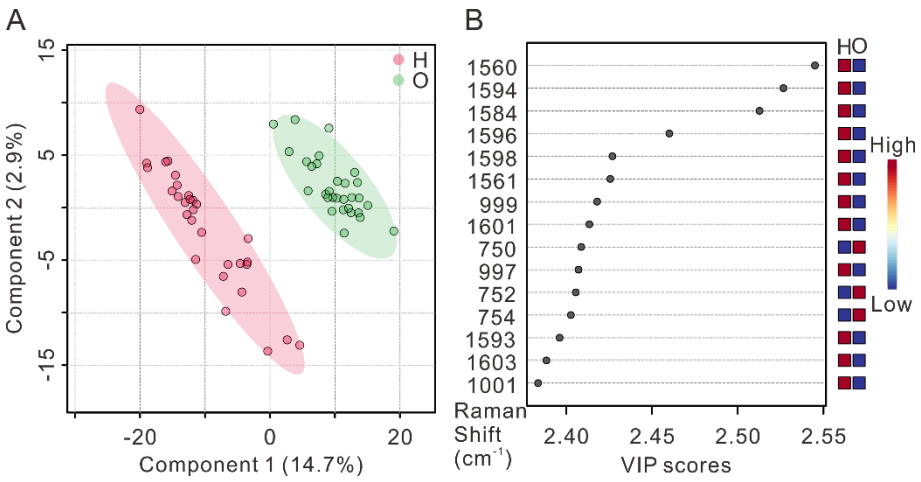

Figure S11. (A) PLS-DA of SERS data of plasma-derived exosomes from 10 healthy controls (H) and 10 osteosarcoma patients (O). Three replicates were performed for each sample. (B) Significant SERS features identified by PLS-DA from plasma-derived exosomes from the 10 healthy controls (H) and 10 osteosarcoma patients (O).

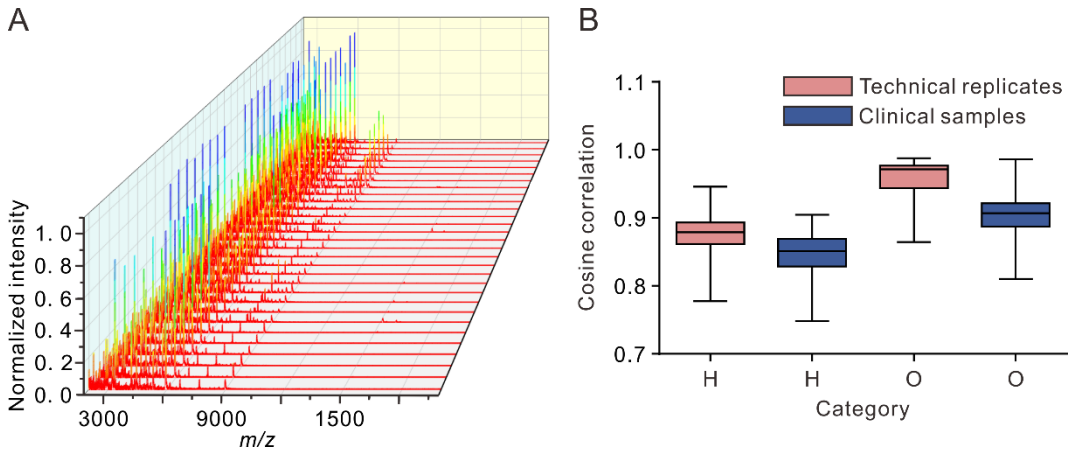

Figure S12. (A) The graph represents 30 representative MALDI-TOF mass spectra of plasma-derived exosomes isolated from 10 osteosarcoma patients. Three replicates were performed for each sample. The adjacent three mass spectra were from the same sample. (B) Cosine correlation of MALDI-TOF mass spectra of plasma-derived exosomes isolated from 10 healthy controls (H) or 10 osteosarcoma patients (O). Three replicates were performed for each sample. The red box-plots represent the distribution of cosine correlation between technical replicates of each sample. The blue box-plots represent the distribution of cosine correlation of MALDI-TOF mass spectra of different clinical samples. The boxes show interquartile ranges (IQR), and the whiskers show 95% percentiles; no outliers are shown.

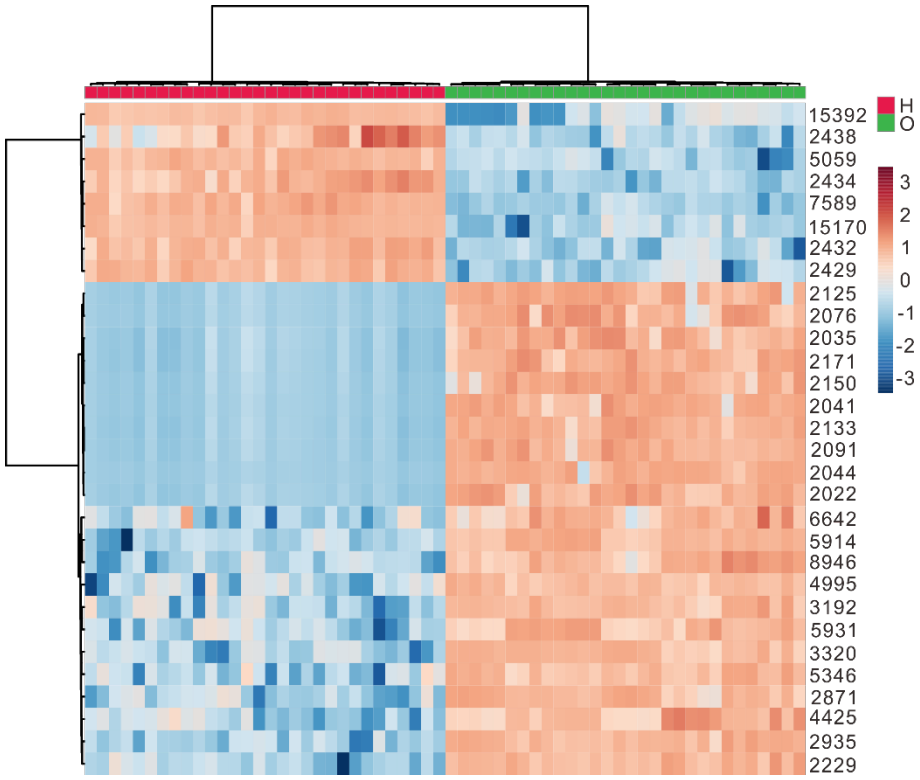

Figure S13. Hierarchical clustering of the MALDI-TOF mass spectra of plasma-derived exosomes isolated from 10 healthy controls (H) and 10 osteosarcoma patients (O) shown as heatmap using Euclidean distance measure and Ward linkage. Three replicates were performed for each sample.

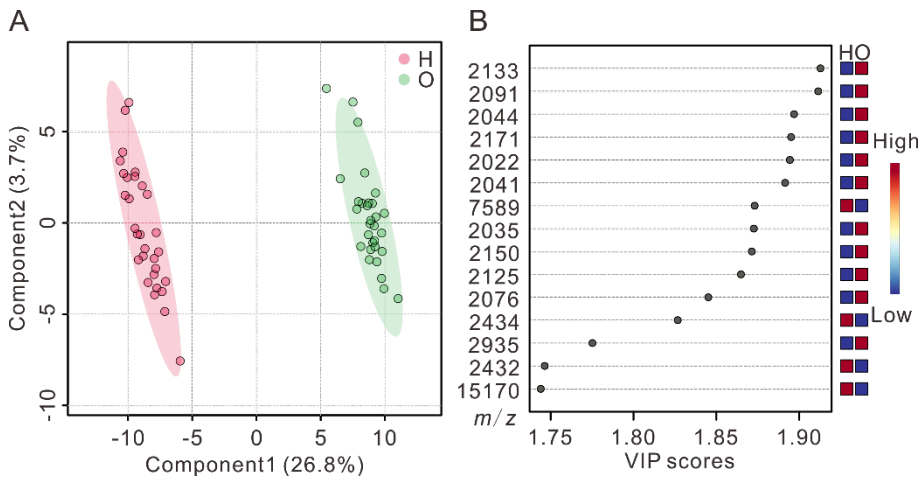

Figure S14. (A) PLS-DA of MALDI-TOF mass spectra of plasma-derived exosomes from 10 healthy controls (H) and 10 osteosarcoma patients (O). Three replicates were performed for each sample. (B) Important MALDI-TOF MS features identified by PLS-DA from plasma-derived exosomes from 10 healthy controls (H) and 10 osteosarcoma patients (O).

Table S1. Assignments of the major SERS peaks of the plasma-derived exosomes from a healthy control and an osteosarcoma patient.

Healthy plasma exosome (cm^{-1})	Osteosarcoma Plasma exosomes (cm^{-1})	Major peak assignment	Ref.
570		Carbohydrate present in cell membrane	1
642	646	Tyrosine	2
651		Tyrosine	2
668	668	T, G(DNA/RNA)	3
747	751	Adenine (Nucleic acids)	4
838	822	Tyrosine	2
892		Stretching (O-C-C-N+), Stretching (C_4-N+) (Phospholipids)	4
950		N-C_α-C	2
984		Tyrosine, Valine	2
1004	1004	Phenylalanine	2
1071		Lipids and nucleic acids (cytosine, guanine, adenine)	5
	1078	C–C or C–O stretch (lipid) C–C or PO_2 stretch (nucleic acids)	5
1101	1101	Phosphodioxy sym-stretching (PO_2^-) (Nuleic acids)	4
1128		Proteins: stretching C-N; Carbohydrates: stretching C-O	2, 6
1145	1150	Lipids and nucleic acids (cytosine, guanine, adenine)	5
1219	1219	U, C ring; sugar puckering (Nuleic acids)	4
1244	1244	Amide III (β-Sheet)	6
1257		U, C ring; sugar puckering (Nuleic acids)	4
1289	1293	Amide III-collagen	5
1336	1336	Proteins: twisting (CH_2, CH_3)	6
1362	1362	Pyrimidine and imidazole rings (Nuleic acids)	4
	1374	Pyrimidine and imidazole rings A/G stacking (Nuleic acids)	4
1402	1402	Deformation CH_3; asym-Stretching COO^-	6
1410		DNA bases	
1465	1465	C-H (deformation)	2
1538		Polyene stretching (C=C) (Carotenoids)	4
1655	1655	Amide I protein band	7
	1684	Stretching (C=C) (Amide I)	8
1723		Ester C=O stretch (lipid)	4

Reference

1. J. Sundaram, B. Park, A. Hinton, K. C. Lawrence and Y. Kwon, *J. Food Meas. Charact.*, 2013, **7**, 1-12.
2. A. Rygula, K. Majzner, K. M. Marzec, A. Kaczor, M. Pilarczyk and M. Baranska, *J. Raman Spectrosc.*, 2013, **44**, 1061-1076.
3. J. C. Fraire, S. Stremersch, D. Bouckaert, T. Monteyne, T. De Beer, P. Wuytens, R. De Rycke, A. G. Skirtach, K. Raemdonck, S. De Smedt and K. Braeckmans, *ACS Appl. Mater. Interfaces*, 2019, **11**, 39424-39435.
4. S. G. Kruglik, F. Royo, J. M. Guigner, L. Palomo, O. Seksek, P. Y. Turpin, I. Tatischeff and J. M. Falcon-Perez, *Nanoscale*, 2019, **11**, 1661-1679.
5. M. Moreno, L. Raniero, E. Â. L. Arisawa, A. M. do Espírito Santo, E. A. P. dos Santos, R. A. Bitar and A. A. Martin, *Theor. Chem. Acc.*, 2009, **125**, 329-334.
6. V. Shalabaeva, L. Lovato, R. La Rocca, G. C. Messina, M. Dipalo, E. Miele, M. Perrone, F. Gentile and F. De Angelis, *PLoS One*, 2017, **12**, e0175581.
7. A. Gualerzi, S. A. A. Kooijmans, S. Niada, S. Picciolini, A. T. Brini, G. Camussi and M. Bedoni, *J. Extracell. Vesicles*, 2019, **8**, 1568780.
8. S. Feng, S. Huang, D. Lin, G. Chen, Y. Xu, Y. Li, Z. Huang, J. Pan, R. Chen and H. Zeng, *Int. J. Nanomedicine*, 2015, **10**, 537-547.